Chapter 7

The Cosmic Microwave Background

7.1 The isotropic CMB

7.1.1 Thermal history of the Universe

- How does the Universe evolve thermally? We have seen earlier that the abundance of ^{4}He shows that the Universe must have gone through an early phase which was hot enough for the nuclear fusion of light elements. But was there thermal equilibrium? Thus, can we speak of the "temperature of the Universe"?
- from isotropy, we must conclude that the Universe expanded *adiathermally*: no heat can have flowed between any two volume elements in the Universe because any flow would have defined a preferred direction, which is forbidden by isotropy;
- an *adiathermal* process is *adiabatic* if it proceeds slow enough for equilibrium to be maintained; then, it is also *reversible* and *isentropic*;
- of course, irreversible processes such as particle annihilations must have occurred during the evolution of the Universe; however, as we shall see later, the entropy in the Universe is so absolutely dominated by the photons of the microwave background radiation that no entropy production by irreversible processes can have added a significant amount of entropy; thus, we assume that the Universe has in fact expanded *adiabatically*;
- the next question concerns thermal equilibrium; of course, as the Universe expands and cools, particles are diluted and interaction rates drop, so thermal equilibrium must break down at some point for any particle species because collisions become to rare; very

early in the Universe, however, the expansion rate was very high, and it is important to check whether thermal equilibrium can have been maintained *despite* the rapid expansion;

- the collision probability between any two particle species will be proportional to their number densities squared, $\propto n^2$, because collisions are dominated by two-body encounters; the collision *rate*, i.e. the number of collisions experienced by an individual particle with others will be $\propto n$, which is $\propto a^{-3}$ for non-relativistic particles; thus, the collision time scale was $\tau_{\rm coll} \propto a^3$;

- according to Friedmann's equation, the expansion rate in the very early Universe was determined by the radiation density, and thus proportional to $\propto \dot{a}/a \propto a^{-2}$, and the expansion time scale was $\tau_{\rm exp} \propto a^2$;

- equilibrium could be maintained as long as the collision time scale was sufficiently shorter than the expansion time scale,

$$\tau_{\rm coll} \ll \tau_{\rm exp} \ , \tag{7.1}$$

  which is easily achieved in the early Universe when $a \ll 1$; thus, even though the expansion rate was very high in the early Universe, the collision rates were even higher, and thermal equilibrium can have been maintained;

- the final assumption is that the components of the cosmic fluid behave as ideal gases; by definition, this requires that their particles interact with a very short-ranged force, which implies that partition sums can be written as powers of one-particle partition sums and that the internal energy of the fluids does not depend on the volume occupied; this is a natural assumption which holds even for charged particles because they shield opposite charges on length scales small compared to the size of the observable universe;

- it is thus well justified to assume that there was thermal equilibrium between all particle species in the early universe, that the constituents of the cosmic "fluid" can be described as ideal gases, and that the expansion of the universe can be seen as an adiabatic process; in later stages of the cosmic evolution, particle species will drop out of equilibrium when their interaction rates fall below the expansion rate of the Universe;

- as long as all species in the Universe are kept in thermodynamic equilibrium, there is a single temperature characterising the cosmic fluid; once particle species freeze out, their temperatures will begin deviating; even then, we characterise the thermal evolution of the Universe by the temperature of the photon background;

7.1.2 Mean properties of the CMB

- as discussed before, the CMB had been predicted in order to explain the abundance of the light elements, in particular of ^{4}He; it was serendipitously discovered by Penzias and Wilson in 1965;

- measurements of the energy density in this radiation were mostly undertaken at long (radio) wavelengths, i.e. in the Rayleigh-Jeans part of the CMB spectrum; to firmly establish that the spectrum is indeed the Planck spectrum expected for thermal black-body radiation, the FIRAS experiment was placed on-board the COBE satellite, where it measured the best realisation of a Planck spectrum ever observed;

- we shall see shortly that the mere fact that the CMB does indeed have a Planck spectrum lends strong support to the cosmological standard model; the temperature of the Planck curve best fitting the latest measurement of the CMB spectrum by the WMAP satellite is

$$T_0 = 2.726\,\mathrm{K}\,, \tag{7.2}$$

  which implies a mean number density of CMB photons of

$$n_{\mathrm{CMB}} = 405\,\mathrm{cm}^{-3} \tag{7.3}$$

  and an energy density in the CMB of

$$u_{\mathrm{CMB}} = 4.2 \times 10^{-13}\,\mathrm{erg\,cm}^{-3}\,, \tag{7.4}$$

  which corresponds to a mass density of

$$\rho_{\mathrm{CMB}} = 4.7 \times 10^{-34}\,\mathrm{g\,cm}^{-3}\,; \tag{7.5}$$

- the density parameter of the CMB radiation is thus

$$\Omega_{\mathrm{r0}} = 4.8 \times 10^{-5}\,, \tag{7.6}$$

  which shows that the scale factor at matter-radiation equality was

$$1/a_{\mathrm{eq}} = \frac{\Omega_{\mathrm{m0}}}{\Omega_{\mathrm{r0}}} \approx 6200\,; \tag{7.7}$$

- the number density of baryons in the Universe is approximately

$$n_{\mathrm{B}} \approx \frac{\Omega_{\mathrm{B0}}\rho_{\mathrm{cr}}}{m_{\mathrm{p}}} \approx 2.3 \times 10^{-7}\,\mathrm{cm}^{-3}\,, \tag{7.8}$$

  confirming that the photon-to-baryon ratio is extremely high,

$$\frac{1}{\eta} \approx \frac{405}{2.3 \times 10^{-7}} \approx 1.8 \times 10^{9}\,; \tag{7.9}$$

7.1.3 Decoupling of the CMB

- When and how was the CMB set free? While the Universe was sufficiently hot to keep electrons and protons separated (we neglect heavier elements here for simplicity), the photons scattered off the charged particles, their mean free path was short, and the photons could not propagate. When the Universe cooled below a certain temperature, electrons and protons combined to form hydrogen, free charges disappeared, the mean free path became virtually infinite and photons could freely propagate.

- the recombination reaction

$$p + e^- \rightarrow H + \gamma \tag{7.10}$$

  can thermodynamically be described by minimising the free energy

$$F = -kT \ln Z = -kT \ln \left[\frac{Z_\mathrm{p}^{N_\mathrm{p}}}{N_\mathrm{p}!} \frac{Z_\mathrm{e}^{N_\mathrm{e}}}{N_\mathrm{e}!} \frac{Z_\mathrm{H}^{N_\mathrm{H}}}{N_\mathrm{H}!} \right] , \tag{7.11}$$

  where Z is the canonical partition sum of the mixture of protons, electrons and hydrogen atoms, while $Z_{\mathrm{p,e,H}}$ are the grand-canonical one-particle partition sums of the protons, the electrons and the hydrogen atoms, respectively, and $N_{\mathrm{p,e,H}}$ are their numbers in a closed subvolume;

- the constant number of baryons is $N_\mathrm{B} = N_\mathrm{p} + N_\mathrm{H}$ and the number of electrons is $N_\mathrm{e} = N_\mathrm{p}$, thus $N_\mathrm{H} = N_\mathrm{B} - N_\mathrm{e}$, and we can express the numbers of all particle species by the number of electrons N_e; finally, the chemical potentials must sum to zero in equilibrium, $\mu_\mathrm{p} + \mu_\mathrm{e} - \mu_\mathrm{H} = 0$;

- then, the equilibrium state is found by extremising the free energy,

$$\frac{\partial F}{\partial N_\mathrm{e}} = 0 , \tag{7.12}$$

  and solving for the electron number N_e or, equivalently, for the ionisation fraction $x = N_\mathrm{e}/N_\mathrm{B}$; the result is Saha's equation

$$\frac{x^2}{1-x} = \frac{\sqrt{\pi}}{4\sqrt{2}\zeta(3)\eta} \left(\frac{m_\mathrm{e} c^2}{kT} \right)^{3/2} \mathrm{e}^{-\chi/kT} \approx \frac{0.26}{\eta} \left(\frac{m_\mathrm{e} c^2}{kT} \right)^{3/2} \mathrm{e}^{-\chi/kT} , \tag{7.13}$$

  where χ is the ionisation energy of hydrogen, $\chi = 13.6\,\mathrm{eV}$, and ζ is the Riemann Zeta function;

- notice that Saha's equation contains the inverse of the η parameter (7.9), which is a huge number due to the high photon-to-baryon ratio in the Universe; this counteracts the exponential which would otherwise guarantee that recombination happens

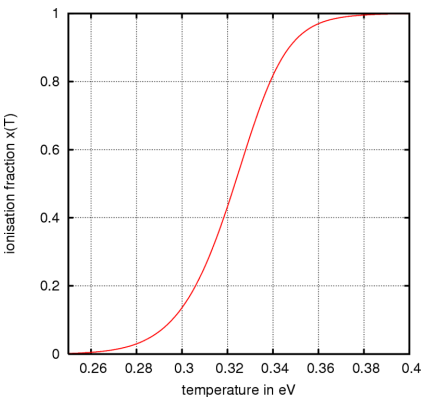

Once recombination sets in, the ionisation fraction x drops very quickly.

when $kT \approx \chi$, i.e. at $T \approx 1.6 \times 10^5\,\mathrm{K}$; recombination is thus delayed by the high photon number, which illustrates that newly formed hydrogen atoms are effectively reionised by sufficiently energetic photons until the temperature has dropped well below the ionsation energy (we saw this also for big bang nucleosynthesis; the epoch of actual nucleosynthesis was delayed until a very long time after the mean temperature of the Universe was $\sim$1 MeV). Putting $x \approx 0.5$ in (7.13) yields a recombination temperature of

$$kT_{\mathrm{rec}} \approx 0.3\,\mathrm{eV}\,, \quad T_{\mathrm{rec}} \approx 3500\,\mathrm{K} \tag{7.14}$$

and thus a recombination redshift of $z_{\mathrm{rec}} \approx 1280$;

- this is well in the matter-dominated phase, and therefore we can estimate the age of the Universe using

$$\begin{aligned} t &= \int_0^a \frac{\mathrm{d}a'}{a'H(a')} \approx \frac{1}{H_0\sqrt{\Omega_{\mathrm{m0}}}} \int_0^a \sqrt{a'}\mathrm{d}a' = \frac{2a^{3/2}}{3H_0\sqrt{\Omega_{\mathrm{m0}}}} \\ &\approx 360,000\,\mathrm{yr}\,; \end{aligned} \tag{7.15}$$

- recombination does not proceed instantaneously; the ionisation fraction x drops from 0.9 to 0.1 within a temperature range of approximately 200 K, corresponding to a redshift range of

$$\Delta z \approx \left.\frac{\mathrm{d}z}{\mathrm{d}T}\right|_{z_{\mathrm{rec}}} \Delta T \approx \left.\frac{\mathrm{d}}{\mathrm{d}T}\left(\frac{T}{T_0} - 1\right)\right|_{z_{\mathrm{rec}}} \Delta T \approx \frac{\Delta T}{T_0} \approx 75\,; \tag{7.16}$$

or a time interval of

$$\Delta t \approx \frac{\Delta a}{aH} \approx \frac{\Delta z}{H_0\sqrt{\Omega_{\mathrm{m0}}}(1+z)^{5/2}} \approx 35,000\,\mathrm{yr}\,; \tag{7.17}$$

- we are thus led to conclude that the CMB was released when the Universe was approximately 360,000 years old, during a phase that lasted approximately 35,000 years; we have derived this result merely using the present temperature of the CMB, the photon-to-baryon ratio, the Hubble constant and the matter density parameter Ω_{m0}; the cosmological constant or a possible curvature of the Universe do not matter here;

- the fact that the temperature of the Universe dropped by $\approx 200\,\mathrm{K}$ while the CMB was released leads to another remarkable realisation: How can the CMB have a Planck spectrum with a *single* temperature if it was released from a plasma with a fairly broad *range of temperatures*? In a Friedmann-Lemaître model universe, this is easy to understand: Photons released from higher-temperature plasma were released somewhat earlier and were subsequently redshifted by a somewhat larger amount. The range

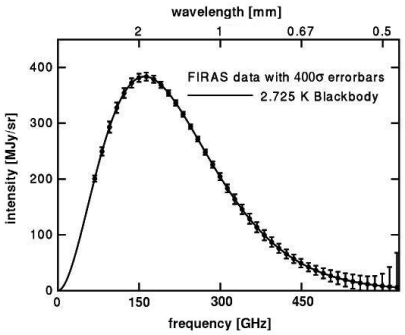

The FIRAS instrument on-board the COBE satellite confirmed that the CMB has the most perfect Planck spectrum ever measured.

of temperatures is thus precisely compensated by the redshift, which confirms the expectation that $T \propto a^{-1}$ in Friedmann-Lemaître models. Thus, the fact that the CMB has a Planck spectrum with a single temperature indirectly confirms that we are living in a Friedmann-Lemaître universe.

7.2 Structures in the CMB

7.2.1 The dipole

- the Earth is moving around the Sun, the Sun is orbiting around the Galactic centre, the Galaxy is moving within the Local Group, which is falling towards the Virgo cluster of galaxies; we can thus not expect that the Earth is at rest with respect to the CMB; we denote the net velocity of the Earth with respect to the CMB rest frame by $v_\oplus$;

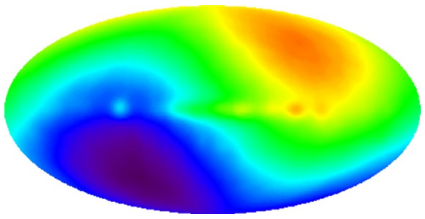

The Earth's motion with respect to the CMB rest frame imprints a dipolar temperature pattern on the CMB with milli-Kelvin ampitude.

- Lorentz transformation shows that, to lowest order in $v_\oplus/c$, the Earth's motion imprints a dipolar intensity pattern on the CMB with an amplitude of

$$\frac{\Delta T}{T_0} = \frac{v_\oplus}{c} \; ; \tag{7.18}$$

the dipole's amplitude has been measured to be $\approx 1.24\,m\mathrm{K}$, from which the Earth's velocity is inferred to be

$$v_\oplus \approx 371\,\mathrm{km\,s^{-1}} \; ; \tag{7.19}$$

- this is the highest-order deviation from isotropy in the CMB, but it is irrelevant for our purposes since it does not allow any conclusions on the Universe at large;

7.2.2 Expected amplitude of CMB fluctuations

- it is reasonable to expect that density fluctuations in the CMB should match density fluctuations in the matter because photons were tightly coupled to baryons by Compton scattering before recombination; since the radiation density is $\propto T^4$, a density contrast δ is expected to produce relative temperature fluctuations of order

$$\delta = \frac{\delta\rho}{\rho} - 1 \approx \frac{4T^3\delta T}{T^4} - 1 \quad \Rightarrow \quad \frac{\delta T}{T} \approx \frac{1+\delta}{4} \; ; \tag{7.20}$$

- obviously, there are large-scale structures in the Universe today whose density contrast reaches or even substantially exceeds unity; assuming linear structure growth on large scales, and

knowing the scale factor of recombination, we can thus infer that relative temperature fluctuations of order

$$\frac{\delta T}{T} \approx \frac{1}{4}\left(1 + \frac{1}{D_+(a_{\rm rec})}\right) \approx \frac{1}{4a_{\rm rec}} \approx 10^{-3} \qquad (7.21)$$

should be seen in the CMB, i.e. fluctuations of order mK, similar to the dipole; such fluctuations, however, were not observed, although cosmologists kept searching increasingly desperately for decades after 1965;

- Why do they not exist? The estimate above is valid only under the assumption that matter and radiation were tightly coupled. Should this not have been the case, density fluctuations did not need to leave such a pronounced imprint on the CMB. In order to avoid the tight coupling, the majority of matter must not interact electromagnetically. Thus, we conclude from the absence of mK fluctuations in the CMB that matter in the Universe must be dominated by something that does not interact with light. This is perhaps the strongest argument in favour of dark matter.

7.2.3 Expected CMB fluctuations

- before we come to the results of CMB observations and their significance for cosmology, let us summarise which physical effects we expect to imprint structures on the CMB;

- the basic hypothesis is that the cosmic structures that we see today formed via gravitational instability from seed fluctuations in the early Universe, whose origin is yet unclear; this implies that there had to be density fluctuations at the time when the CMB was released; via Poisson's equation, these density fluctuations were related to fluctuations in the Newtonian potential;

Sachs-Wolfe Effect

- photons released in a potential fluctuation $\delta\Phi$ lost energy if the fluctuation was negative, and gained energy when the fluctuation was positive; this energy change can be translated to the temperature change

$$\frac{\delta T}{T} = \frac{1}{3}\frac{\delta\Phi}{c^2}\,, \qquad (7.22)$$

which is called the Sachs-Wolfe effect after the people who first described it;

- let us briefly look into the expected statistics of the Sachs-Wolfe effect; we introduced the power spectrum of the density fluctuations in (2.22) as the variance of the density contrast in Fourier space; Fourier-transforming Poisson's equation, we see that

$$\delta\hat{\Phi} \propto -\frac{\hat{\delta}}{k^2} \,, \tag{7.23}$$

  and thus the power spectrum of the temperature fluctuations due to the Sachs-Wolfe effect is determined by

$$P_T \propto P_\Phi \propto \frac{\langle\hat{\delta}\hat{\delta}^*\rangle}{k^4} \propto \frac{P_\delta}{k^4} \propto \begin{cases} k^{-3} & k \ll k_0 \\ k^{-7} & k \gg k_0 \end{cases} \tag{7.24}$$

  according to (2.23); this shows that the Sachs-Wolfe effect can only be important at small k, i.e. on large scales, and dies off quickly towards smaller scales;

Acoustic Oscillations

- the cosmic fluid consisted of dark matter, baryons and photons; overdensities in the dark matter compressed the fluid due to their gravity until the rising pressure in the tightly coupled baryon-photon fluid was able to counteract gravity and drove the fluctuations apart; in due course, the pressure sank and gravity won again, and so forth: the cosmic fluid thus underwent acoustic oscillations;

- since the pressure was dominated by the photons, whose pressure is a third of their energy density, the sound speed was

$$c_\mathrm{s} \approx \sqrt{\frac{p}{\rho}} = \frac{c}{\sqrt{3}} \approx 0.58\,c \;; \tag{7.25}$$

- only such density fluctuations could undergo acoustic oscillations which were small enough to be crossed by sound waves in the available time; we saw before that recombination happened when the Universe was $\approx 360,000\,\mathrm{yr}$ old, so the largest length that could be traveled by sound wave was the *sound horizon*

$$r_\mathrm{s} \approx 360,000\,\mathrm{yr} \times \frac{c}{\sqrt{3}} \approx 63\,\mathrm{kpc} \;; \tag{7.26}$$

  larger-scale density fluctuations could not oscillate;

- we saw in (2.15) that the angular-diameter distance from today to scale factor $a \ll 1$ is

$$D_\mathrm{ang}(a) = \frac{ca}{H_0} \int_a^1 \frac{\mathrm{d}x}{x^2 E(x)} \tag{7.27}$$

if we assume for simplicity that the universe is spatially flat; then, the denominator in the integrand is

$$x^2 E(x) = \sqrt{\Omega_{\rm m0} x + (1-\Omega_{\rm m0}) x^4} = \sqrt{\Omega_{\rm m0} x} \sqrt{1 + \frac{1-\Omega_{\rm m0}}{\Omega_{\rm m0}} x^3} \tag{7.28}$$

- inserting, we find that we can approximate the angular-diameter distance for $a \ll 1$ by

$$D_{\rm ang}(a_{\rm rec}) \approx \frac{2 c a_{\rm rec}}{H_0 \sqrt{\Omega_{\rm m0}}} \left(1 - \frac{1-\Omega_{\rm m0}}{6\Omega_{\rm m0}}\right) \approx 7.3\,{\rm Mpc}\ , \tag{7.29}$$

and the sound horizon sets an angular scale of

$$\theta_{\rm s} = \frac{2 r_{\rm s}}{D_{\rm ang}(a_{\rm rec})} \approx 1^\circ\ , \tag{7.30}$$

to which we shall shortly return;

- inserting the time directly from (7.15), the sound speed from (7.25) and the angular-diameter distance from (7.29) reveals a weak dependence of $\theta_{\rm s}$ on $\Omega_{\rm m0}$ even for a flat Universe,

$$\theta_{\rm s} \approx \frac{2 a_{\rm rec}^{1/2}}{3\sqrt{3}} \left(1 + \frac{1-\Omega_{\rm m0}}{6\Omega_{\rm m0}}\right)\ ; \tag{7.31}$$

Silk Damping

- a third effect influencing structures in the CMB is caused by the fact that, as recombination proceeds, the mean-free path of the photons increases; if $n_{\rm e} = x n_{\rm B}$ is the electron number density and $\sigma_{\rm T}$ is the Thomson cross section, the mean-free path is

$$\lambda \approx \frac{1}{x n_{\rm B} \sigma_{\rm T}}\ ; \tag{7.32}$$

as the ionisation fraction x drops towards zero, the mean-free path aproaches infinity;

- after N scatterings, the photons will have diffused by

$$\lambda_{\rm D} \approx \sqrt{N}\lambda\ ; \tag{7.33}$$

the number of scatterings per unit time is

$${\rm d}N \approx x n_{\rm B} \sigma_{\rm T} c {\rm d}t\ , \tag{7.34}$$

and thus the diffusion scale is given by

$$\lambda_{\rm D}^2 \approx \int \lambda^2 {\rm d}N \approx \int \frac{c {\rm d}t}{x n_{\rm B} \sigma_{\rm T}}\ ; \tag{7.35}$$

- the latter integral is dominated by the short recombination phase during which x drops to zero; inserting $x \approx 1/2$ as a typical value, we can thus approximate

$$\lambda_{\mathrm{D}}^2 \approx \frac{2c\Delta t}{n_{\mathrm{B}}\sigma_{\mathrm{T}}} \; ; \tag{7.36}$$

- around recombination, the baryon number density is

$$n_{\mathrm{B}} \approx \frac{\Omega_{\mathrm{B0}}\rho_{\mathrm{cr}}}{m_{\mathrm{p}}a_{\mathrm{rec}}^{-3}} \approx 500\,\mathrm{cm}^{-3} \; , \tag{7.37}$$

  and we find

$$\lambda \approx 2\,\mathrm{kpc} \quad \text{and} \quad \lambda_{\mathrm{D}} \approx 4.5\,\mathrm{kpc} \tag{7.38}$$

  from Eqs. (7.32) and (7.36), respectively; λ_{D} thus corresponds to an angular scale of $\theta_{\mathrm{D}} \approx 5'$ on the sky; this damping mechanism is called *Silk damping* after its discoverer;

- we thus expect three mechanisms to shape the appearance of the microwave sky: the Sachs-Wolfe effect on the largest scales, the acoustic oscillations on scales smaller than the sound horizon, and Silk damping on scales smaller than a few arc minutes;

7.2.4 CMB polarisation

- if the CMB does indeed arise from Thomson scattering, interesting effects must arise from the fact that the Thomson scattering cross section is polarisation sensitive and can thus produced linearly polarised from unpolarised radiation;

- suppose an electron is illuminated by unpolarised radiation from the left, then the radiation scattered towards the observer will be linearly polarised in the perpendicular direction; likewise, unpolarised radiation incoming from the top will be linearly polarised horizontally after being scattered towards the observer;

- thus, if the electron is irradiated by a quadrupolar intensity pattern, the scattered radiation will be partially linearly polarised; the polarised intensity is expected to be of order 10% of the total intensity;

- the polarised radiation must reflect the same physical effects as the unpolarised radiation, and the two must be cross-correlated; much additional information on the physical state of the early Universe should thus be contained in the polarised component of the CMB, besides that a detection of the polarisation would add confirmation to the physical picture of the CMB's origin;

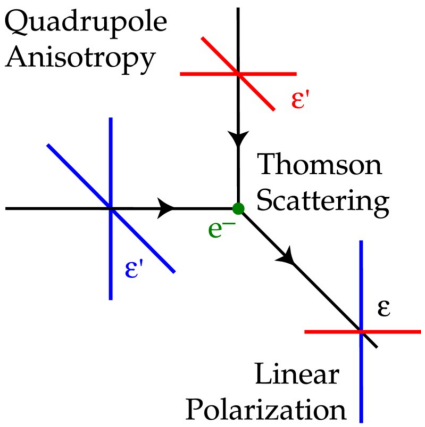

The anisotropy of Thomson scattering causes the CMB to be partially linearly polarised.

7.2.5 The CMB power spectrum

- Fourier transformation is not possible on the sphere, but the analysis of the CMB proceeds in a completely analogous way by decomposing the relative temperature fluctuations into spherical harmonics, finding the spherical-harmonic coefficients

$$a_{lm} = \int \mathrm{d}^2\theta \, \frac{\delta T}{T} \, Y_{lm}(\vec{\theta}) \,, \tag{7.39}$$

  and from them the power spectrum

$$C_l \equiv \frac{1}{2l+1} \sum_{m=-l}^{l} |a_{lm}|^2 \,, \tag{7.40}$$

  which is equivalent to the matter power spectrum (2.22) on the sphere; the average over m expresses the expectation of statistical isotropy;

- the shape of the CMB power spectrum reflects the three physical mechanisms identified above: at small l (on large scales), the Sachs-Wolfe effect causes a feature-less plateau, followed by pronounced maxima and minima due to the acoustic oscillations, damped on the smallest scales (largest l) by Silk damping;

- the detailed shape of the CMB power spectrum depends sensitively on the cosmological parameters, which can in turn be determined by fitting the theoretically expected to the measured C_l; this is the main reason for the detailed and sensitive CMB measurements pioneered by COBE, continued by ground-based and balloon experiments, and culminating recently in the spectacular results obtained by the WMAP satellite;

7.2.6 Microwave foregrounds

- by definition, the CMB is the oldest visible source of photons because all possible earlier sources could not shine through the hot cosmic plasma; therefore, every source that produced microwave photons since, or that produced photons which became redshifted into the microwave regime by now, must appear superposed on the CMB; the CMB is thus hidden behind curtains of foreground emission that have to be opened before the CMB can be observed;

- broadly, the CMB foregrounds can be grouped into point sources and diffuse sources; the most important among the point sources are infrared galaxies at high redshift, galaxy clusters affecting the CMB through the Sunyaev-Zel'dovich effect, and bodies in the Solar System such as the major planets, but even some of the asteroids;

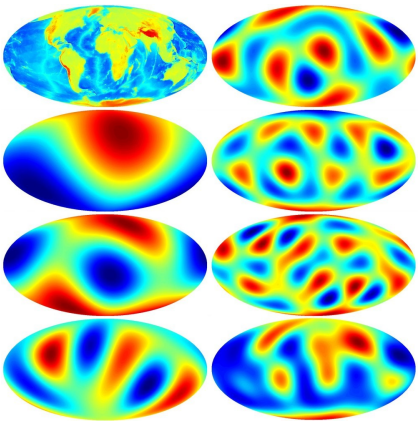

The Earth's surface, and its lowest-order multipoles: dipole, quadrupole and octupole (left column below the map), and the multipoles with $l = 4 \ldots 7$ (right column).

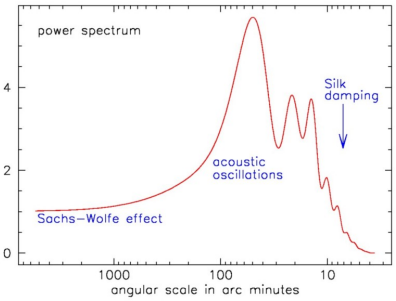

The CMB power spectrum is characterised by three physical effects: the Sachs-Wolfe effect, acoustic oscillations, and Silk damping.

- the population of infrared sources at high redshift is poorly known, but the angular resolution of CMB measurements has so far been too low to be significantly contaminated by them; future CMB observations will have to remove them carefully;

- the Sunyaev-Zel'dovich effect was introduced under 3.3 before; once the angular resolution of CMB detectors will drop towards a few arc minutes, a large number of galaxy clusters are expected to be discovered by their peculiar spectral signature, casting a shadow below, emitting above, and vanishing at 217 GHz; the Sunyaev-Zel'dovich effect comes in two variants; one is the *thermal* effect discussed above, the other is the *kinetic* effect caused by the bulk motion of the cluster as a whole, which causes CMB radiation to be scattered by the electrons moving with the cluster; very few clusters have so far been detected in CMB data, but thousands are expected to be found in future missions;

- microwave radiation from bodies in the Solar System has so far been used to calibrate microwave detectors; CMB observations at an angular resolution below $\sim 10'$ are expected to detect hundreds of minor planets;

- diffuse CMB foregrounds are mainly caused by our Galaxy itself; there are three main components: synchrotron emission, emission from warm dust, and *bremsstrahlung*;

- synchrotron radiation is emitted by relativistic electrons in the Galaxy's magnetic field; it is highly linearly polarised and has a power-law spectrum falling steeply from radio towards microwave frequencies; it is centred on the Galactic plane, but shows filamentary extensions from the Galactic centre towards the Galactic poles;

- the dust in the Milky Way is also concentrated in the Galactic plane; it is between $10 \ldots 20\,\mathrm{K}$ warm and therefore substantially warmer than the CMB itself; it has a Planck spectrum which is self-absorbed due to the high optical depth of the dust; due to its higher temperature, the dust has a spectrum rising with increasing frequency in the frequency window in which the CMB is usually observed;

- *bremsstrahlung* radiation is emitted by ionised hydrogen clouds (HII regions) in the Galactic plane; it has the typical, exponentially-falling spectrum of thermal free-free radiation; further sources of microwave radiation in the Galaxy are less prominent; among them are line emission from CO molecules embedded in cool gas clouds;

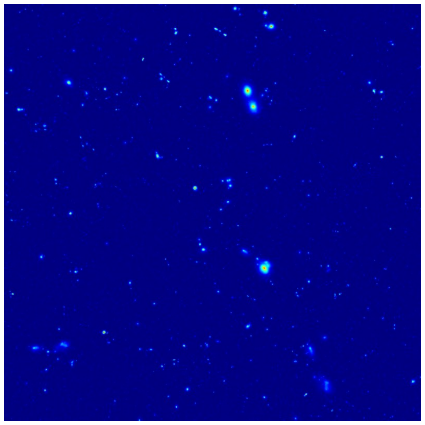

Galaxy clusters appear as characteristic point-like sources on the CMB.

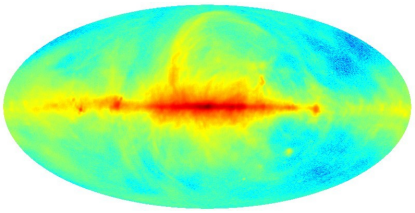

Relativistic electrons gyrating in the Galaxy's magnetic field emit synchrotron radiation.

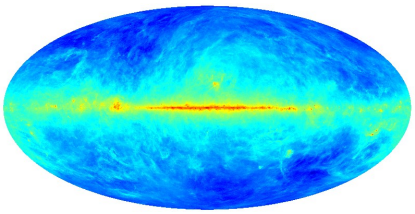

Warm dust in the galaxy also adds to the microwave foregrounds.

- the falling spectra of the synchrotron and free-free radiation, and the rising spectrum of the dust create a window for CMB observations between $\sim 100 \ldots 200\,\mathrm{GHz}$; the different spectra of the foregrounds, and their non-Planckian character, are crucial for their proper removal from the CMB data; therefore, CMB measurements have to be carried out in multiple frequency bands;

7.2.7 Measurements of the CMB

- Wien's law shows that the CMB spectrum peaks at $\lambda_{\mathrm{max}} \approx 0.11\,\mathrm{cm}$, or at a frequency of $\nu_{\mathrm{max}} \approx 282\,\mathrm{GHz}$;
- as we saw, Silk damping sets in below a few arc minutes, thus most of the structures in the CMB are resolvable for rather small telescopes; according to the formula

$$\Delta\theta \approx 1.44\,\frac{\lambda}{D} \tag{7.41}$$

  relating the angular resolution $\Delta\theta$ to the ratio between wavelength and telescope diameter D, we find that mirrors with

$$D \lesssim 1.44\,\frac{\lambda_{\mathrm{max}}}{\theta_{\mathrm{D}}} \approx 75\,\mathrm{cm} \tag{7.42}$$

  are sufficient (recall that θ_{D} needs to be inserted in radians here);
- thus, detectors are needed which are sensitive to millimetre and sub-mm radiation and reach μK sensitivity, while the telescope optics can be kept rather small and simple;
- two types of detector are commonly used; the first are bolometers, which measure the energy of the absorbed radiation by the temperature increase it causes; therefore, they have to be cooled to very low temperatures typically in the mK regime; the second are so-called *high electron mobility detectors* (HEMTs), in which the currents caused by the incoming electromagnetic field are measured directly; the latter detectors measure amplitude and phase of the waves and are thus polarisation-sensitive by construction, which bolometers are not; polarisation measurements with bolometers is possible with suitably shaped so-called *feed horns* guiding the radiation into the detectors;
- since water vapor in the atmosphere both absorbs and emits microwave radiation through molecular lines, CMB observations need to be carried out either at high, dry and cold sites on the ground (e.g. in the Chilean Andes or at the South Pole), or from balloons rising above the troposphere, or from satellites in space;

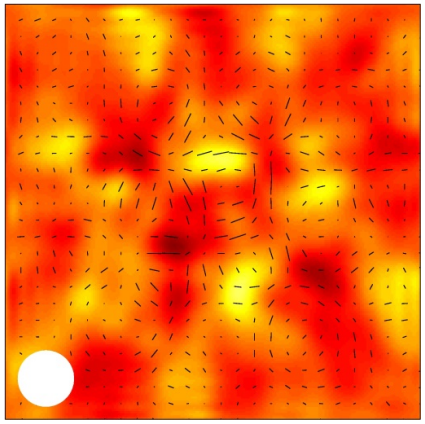

Microwave observations from the ground require cold and dry sites. The Boomerang experiment was

- after the breakthrough achieved with COBE, progress was made with balloon experiments such as *Boomerang* and *Maxima*, and with ground-based interferometers such as *Dasi* (*Degree Angular Scale Interferometer*), *VSA* (*Very Small Array*) and *CBI* (*Cosmic Background Imager*); the balloons covered a small fraction of the sky (typically $\sim$ 1%) at frequencies between 90 and 400 GHz, while the interferometers observe even smaller fields at somewhat lower frequencies (typically around 30 GHz);

- the first discovery of the CMB polarisation and its cross-correlation with the CMB temperature was achieved in 2003 with the *Dasi* interferometer;

- the existence, location and height of the first acoustic peak had been firmly established before the NASA satellite *Wilkinson Microwave Anisotropy Probe* (WMAP for short) was launched, but the increased sensitivity and the full-sky coverage of WMAP produced breath-taking results; WMAP is still operating, measuring the CMB temperature at frequencies between 23 and 94 GHz with an angular resolution of $\gtrsim 15'$; the sensitivity of WMAP is barely high enough for polarisation measurements;

- by now, data from the first five years of operation have been published, and cosmological parameters have been obtained fitting theoretically expected to the measured temperature-fluctuation power spectrum and the temperature-polarisation power spectrum; results are given in the following table:

CMB temperature	T_{CMB}	$2.728 \pm 0.004\,\mathrm{K}$
total density	Ω_{tot}	$0.99^{+0.01}_{-0.01}$
matter density	Ω_{m0}	$0.25^{+0.01}_{-0.01}$
baryon density	Ω_{b0}	$0.043^{+0.001}_{-0.001}$
cosmological constant	$\Omega_{\Lambda 0}$	0.74 ± 0.03
decoupling redshift	z_{dec}	1089 ± 1
age of the Universe	t_0	$13.7 \pm 0.2\,\mathrm{Gyr}$
age at decoupling	t_{dec}	$379^{+8}_{-7}\,\mathrm{kyr}$
power-spectrum normalisation	σ_8	$0.80^{+0.04}_{-0.04}$

- the Hubble constant is *not* an independent measurement from the CMB alone; only by *assuming* a flat universe, it can be inferred from the location of the first acoustic peak in the CMB power spectrum to be $H_0 = 73 \pm 3\,\mathrm{km\,s^{-1}\,Mpc^{-1}}$, which agrees perfectly with the results of the Hubble Key Project and gravitational-lens time delays;

- a European CMB satellite mission is under way: ESA's *Planck* satellite is expected to be launched in 2009; it will observe the microwave sky in ten frequency bands between 30 and 857 GHz

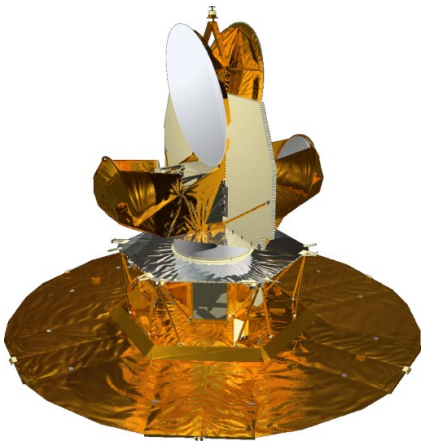

The COBE (top) and WMAP satellites.

with about ten times higher sensitivity than WMAP, and an angular resolution of $\gtrsim 5'$; its wide frequency coverage will be very important for substantially improved foreground subtraction; also, it will have sufficient sensitivity to precisely measure the CMB polarisation in some of its frequency bands; moreover, it is expected that *Planck* will detect of order 10,000 galaxy clusters through their thermal Sunyaev-Zel'dovich effect;

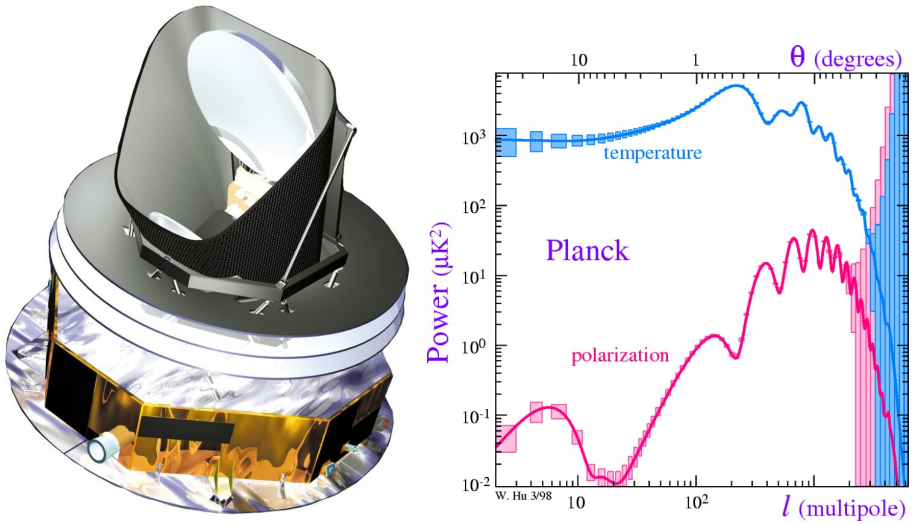

Figure 7.1: The European Planck satellite, to be launched in 2008 (left), and the expected error bars on the temperature and polarisation power spectra (right).

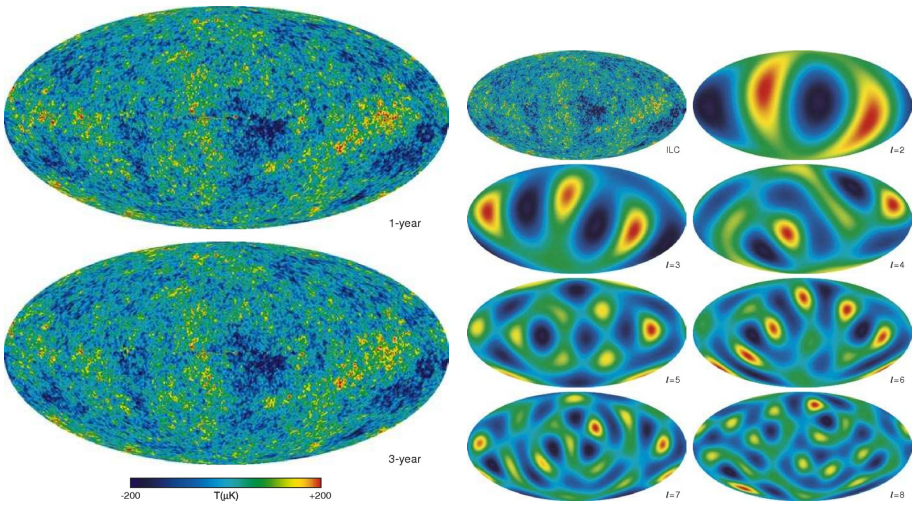

Figure 7.2: *Left*: Comparison between the WMAP temperature maps obtained after one (top) and three years of measurement. *Right*: Decomposition of the WMAP 3-year temperature map into low-order multipoles.

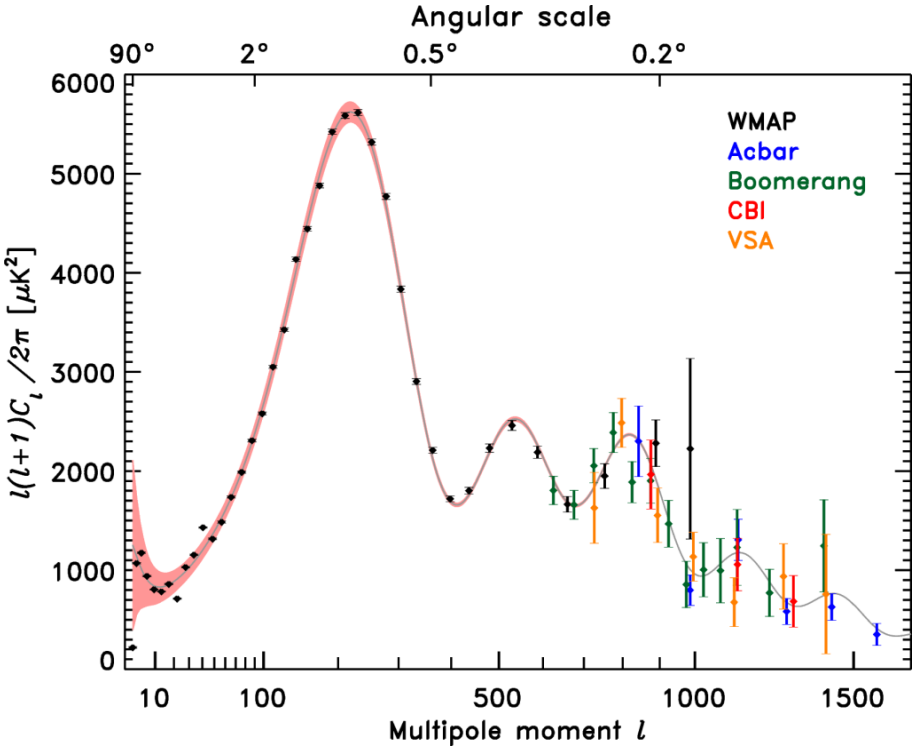

Figure 7.3: Power spectrum of CMB temperature fluctuations as measured from the 3-year data of WMAP and several additional ground-based experiments.

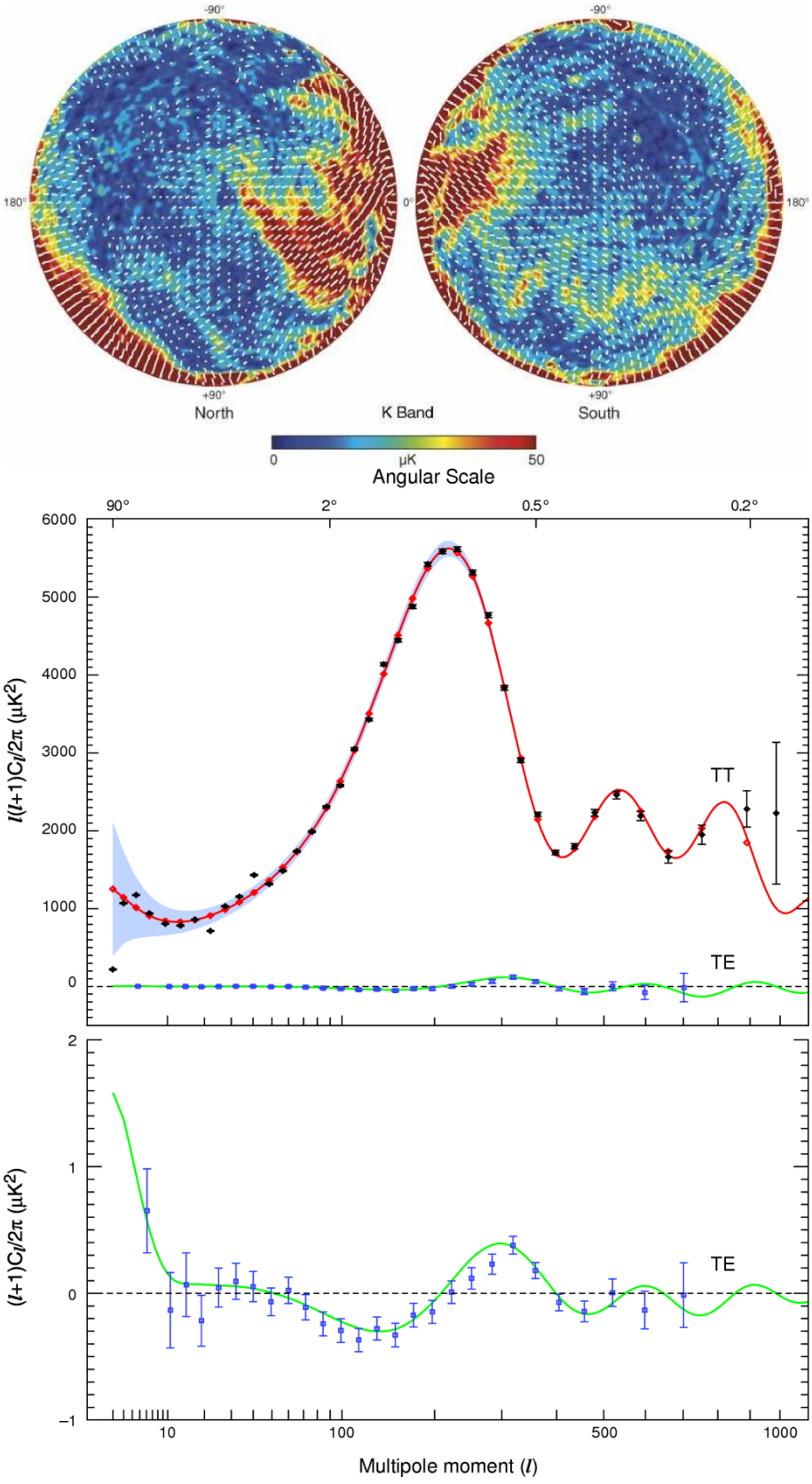

Figure 7.4: *Top*: Polarisation map obtained by WMAP. *Bottom*: The temperature-fluctuation power spectrum (top) and the temperature-polarisation cross-power spectrum determined from the WMAP 3-year data.

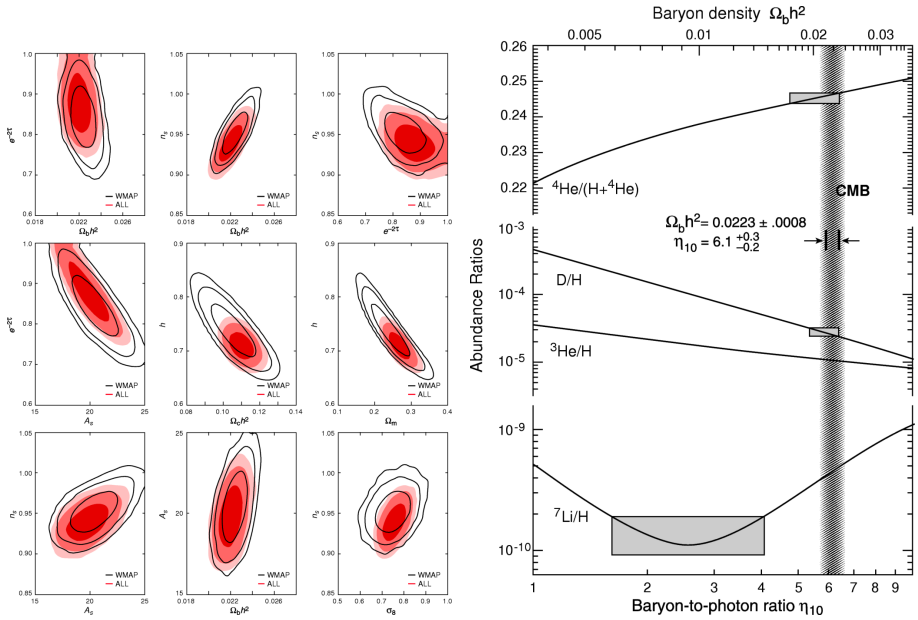

Figure 7.5: *Left*: Constraints on cosmological parameters derived from WMAP 3-year data alone (black contours), and combined with other cosmological data sets (red islands). *Right*: Constraints on the baryon density from primordial nucleosynthesis (vertical grey bar) and from the CMB. The agreement is extraordinary.